Novel Heme Ligation in a *c*-type Cytochrome Involved in Thiosulfate Oxidation: EPR and MCD of SoxAX from *Rhodovulum sulfidophilum*†

Myles R. Cheesman,*,‡ Phillip J. Little,§ and Ben C. Berks*,§

School of Chemical Sciences and School of Biological Sciences, Centre for Metalloprotein Spectroscopy and Biology, University of East Anglia, Norwich NR4 7TJ, U.K.

Received January 3, 2001; Revised Manuscript Received July 10, 2001

ABSTRACT: The SoxAX complex of the bacterium *Rhodovulum sulfidophilum* is a heterodimeric *c*-type cytochrome that plays an essential role in photosynthetic thiosulfate and sulfide oxidation. The three heme sites of SoxAX have been analyzed using electronic absorption, electron paramagnetic resonance, and magnetic circular dichroism spectroscopies. Heme-3 in the ferric state is characterized by a Large g_{max} EPR signal and has histidine and methionine axial heme iron ligands which are retained on reduction to the ferrous state. Hemes-1 and -2 both have thiolate plus nitrogenous ligand sets in the ferric state and give rise to rhombic EPR spectra. Heme-1, whose ligands derive from cysteinate and histidine residues, remains ferric in the presence of dithionite ion. Ferric heme-2 exists with a preparation-dependent mixture of two different ligand sets, one being cysteinate/histidine, the other an unidentified pair with a weaker crystal-field strength. Upon reduction of the SoxAX complex with dithionite, a change occurs in the ligands of heme-2 in which the thiolate is either protonated or replaced by an unidentified ligand. Sequence analysis places the histidine/methionine-coordinated heme in SoxX and the thiolate-liganded hemes in SoxA. SoxAX is the first naturally occurring *c*-type cytochrome in which a thiolate-coordinated heme has been identified.

Sulfide and thiosulfate are the most abundant environmentally available forms of reduced inorganic sulfur. Their oxidation to sulfate is the major part of the oxidative half of the global sulfur cycle, and this process can be accomplished biologically either by photosynthetic Sulfur Bacteria, which use the sulfur compounds as the reductant for carbon dioxide fixation, or by chemotrophic Sulfur Bacteria that additionally use the sulfur compounds as respiratory electron donors (*1*, *2*). However, our knowledge of the molecular processes underlying this ancient metabolism is extremely limited in comparison, for example, to our understanding of the bacterial metalloenzymes involved in the nitrogen cycle. The TOMES (thiosulfate-oxidizing multi-enzyme system) or Sox mechanism is the best characterized pathway of thiosulfate oxidation. This pathway occurs in two phylogenetically distinct groups of photosynthetic Sulfur Bacteria and in many facultatively chemolithotrophic nonphotosynthetic bacteria (*2*−*6*). In the TOMES mechanism, thiosulfate oxidation is thought to proceed via enzyme-bound intermediates (*7*). Sulfide oxidation by these bacteria can also involve elements of the TOMES pathway (*5*, *7*, *8*).

One essential component of TOMES is a hemoprotein encoded by the *soxA* gene (*2*, *4*, *6*, *9*, *10*). The reaction catalyzed by SoxA is uncertain but may, on the basis that alternative functions in thiosulfate metabolism have been assigned to other TOMES components, involve oxidation of sulfur atoms in the zerovalent oxidation state to sulfite. The SoxA protein of the photosynthetic Purple Bacterium *Rhodovulum sulfidophilum* copurifies with a second polypeptide termed SoxX (*6*). The heme cofactors of *R. sulfidophilum* SoxAX are of the covalently linked *c*-type as judged by alkaline pyridine hemochrome spectra (*6*). Sequence analysis of the SoxAX polypeptides together with mass data show that SoxA binds two, and SoxX one, heme groups while analytical ultracentrifugation experiments demonstrate that SoxAX is a heterodimer (*6*). Thus, the SoxAX complex of *R. sulfidophilum* contains three different heme sites.

Here we report a characterization of the heme cofactors of *R. sulfidophilum* SoxAX by electronic absorption, electron paramagnetic resonance (EPR),[1] and magnetic circular dichroism (MCD) spectroscopies at room temperature (RT) and at 4.2 K. Two of the SoxAX heme irons have thiolate/nitrogen coordination while the third heme has methionine/histidine protein ligands. This is the first report of a naturally occurring *c*-type cytochrome with a thiolate heme iron ligand and the first example of two thiolate-coordinated hemes bound to one polypeptide.

† This work was supported by U.K. Biotechnology and Biological Research Council (BBSRC) Grant 83/PO9311 (B.C.B.) and by the BBSRC and Engineering and Physical Sciences Research Council (EPSRC) through core funding to the Centre for Metalloprotein Spectroscopy and Biology (CMSB) under Grant BO1727. P.J.L. was the recipient of a BBSRC studentship.

* Corresponding authors. M.R.C.: tel, +44 (0)1603 592028; fax, +44 (0)1603 592003; e-mail, m.cheesman@uea.ac.uk. B.C.B.: tel, +44 (0)1603 592186; fax, +44 (0)1603 592250; e-mail, b.berks@uea.ac.uk.

‡ School of Chemical Sciences.

§ School of Biological Sciences.

[1] Abbreviations: EPR, electron paramagnetic resonance; MCD, magnetic circular dichroism; UV, ultraviolet; NIR, near-infrared; CT, charge-transfer; RT, room temperature; P450, cytochrome P450; NOS, nitric oxide synthase; CPO, chloroperoxidase; His, histidine; Met, methionine; Lys, lysine; Cys^-, cysteinate.

10.1021/bi0100081 CCC: $20.00
Published on Web 08/10/2001

MATERIALS AND METHODS

Sample Preparation. The thiosulfate-induced multiheme cytochrome c_{551} (SoxAX) was purified from the photosynthetic α-Proteobacterium *Rhodovulum sulfidophilum* DSM 1374^T as described elsewhere (*6*). To record MCD through the 1400−2000 nm region, interference from absorptions caused by vibrational overtones was minimized by preparing samples in deuterium oxide solutions (*11*). These were buffered using 10 mM NaHEPES at pH* 7.0 (pH* is the apparent pH of the solution in D_2O measured using a standard glass electrode). Sodium dithionite solutions were prepared in the same buffer and added to SoxAX solutions in an anaerobic glovebox (Faircrest Engineering, oxygen levels ≤1 ppm in a nitrogen atmosphere). Buffer solutions and SoxAX samples were first stirred in the anaerobic atmosphere to remove traces of oxygen.

Total heme content was determined using the alkaline pyridine hemochrome method (*12*). The SoxAX complex contains three hemes per molecule (*6*), and to reflect this, all spectra are plotted normalized to concentrations equal to one-third of the total heme concentration.

Dithionite-Treated SoxAX. To prepare the sample of dithionite-treated SoxAX, two 1 μL aliquots of 125 mM sodium dithionite in the HEPES buffer solution were sequentially added to the SoxAX sample used for low-temperature MCD spectroscopy. The absorption spectrum was recorded after each addition using a sealed quartz cuvette and showed no further changes upon addition of the second aliquot of sodium dithionite solution. At this point, the sample contained a 37-fold molar excess of sodium dithionite over SoxAX.

Spectroscopic Measurements. Electronic absorption spectra were recorded using Hitachi U3200 and U4001 spectrophotometers. EPR spectra were recorded on an EPR spectrometer comprising an ER-200D electromagnet and microwave bridge interfaced to an EMX control system (Brüker Spectrospin) and fitted with a liquid helium flow cryostat (ESR-9, Oxford Instruments) and a dual-mode X-band cavity (Brüker, type ER4116DM). MCD spectra were recorded using circular dichrographs, JASCO models J-500D and J-730 for the UV−visible and near-infrared regions, respectively. An Oxford Instruments superconducting solenoid with a 25 mm ambient temperature bore was used to generate a magnetic field of 6 T for the room-temperature MCD measurements. Low-temperature MCD measurements were made using an Oxford Instruments SM4 split-coil superconducting solenoid generating a magnetic field of 5 T. Low-temperature MCD intensities ($\Delta\epsilon$) are plotted in units of M^{-1} cm^{-1} at a stated magnetic field which in this work is 5 T. At room temperature, MCD intensities are linearly dependent on magnetic field and are plotted normalized to magnetic field as $\Delta\epsilon/H$ (M^{-1} cm^{-1} T^{-1}). To obtain optical-quality glasses on freezing for low-temperature MCD measurements, glycerol was added to samples to a level of 50% v/v (*11*). That these additions had no effect on the state of the sample was verified by measuring absorption and EPR spectra prior to recording the MCD. Quantitation of low-spin ferric EPR signals was achieved by the integration methods of Aasa and Vängård (*13*) and De Vries and Albracht (*14*) using 1 mM Cu(II)EDTA as a spin concentration standard.

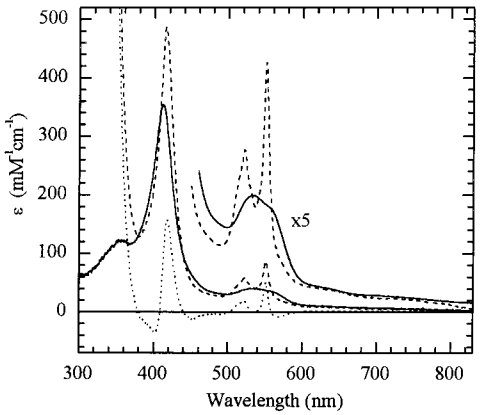

FIGURE 1: Room-temperature electronic absorption spectra of *R. sulfidophilum* SoxAX as prepared oxidized (—), dithionite-treated (− − −), and the (dithionite treated *minus* oxidized) difference spectrum (•••). Buffers were as described under Materials and Methods. Sample concentrations were 8 and 56 μM.

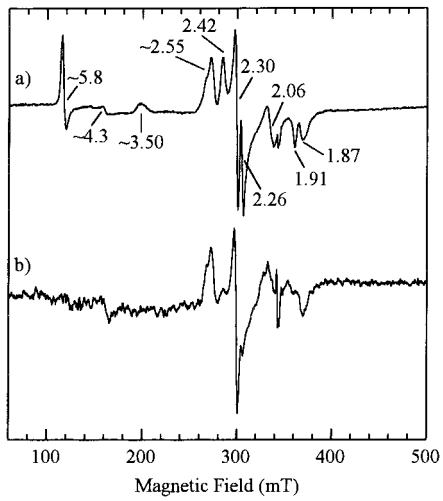

FIGURE 2: X-band EPR spectra of the as-prepared oxidized (a) and dithionite-treated (b) forms of *R. sulfidophilum* SoxAX. Buffers were as described under Materials and Methods. The spectra were recorded at 10 K using 1 mT modulation amplitude and 2 mW microwave power. Sample concentrations were 56 and 55 μM.

RESULTS AND SPECTROSCOPIC ASSIGNMENTS

Electronic Absorption Spectra. The electronic absorption spectrum of oxidized SoxAX (Figure 1, solid line) is typical of low-spin ferric heme. The intensities ($\epsilon_{412.5\ nm} = 350\ mM^{-1}$ cm^{-1}; $\epsilon_{553.5\ nm} = 39.7\ mM^{-1}\ cm^{-1}$) are consistent with the presence of three such species. There is some additional weak intensity to wavelengths longer than 600 nm which will be discussed below.

EPR Spectrum of Oxidized SoxAX. The 10 K X-band EPR spectrum of oxidized SoxAX (Figure 2a) can be assigned to at least three different low-spin ferric heme species as described below. Other signals at $g \sim 5.8$, 4.3, and 2.06 are due to low levels of high-spin ferric heme (*15*), adventitious Fe(III) ion, and adventitious Cu(II) ion, respectively. The $g = 3.50$ peak is the g_z of a Large g_{max} (or Type I) spectrum, one of the two limiting types of normal low-spin ferric heme EPR (*16*, *17*) (the other two *g*-values are often unobservable). Such spectra are known for His/His, His/Met, and His/Lys (or amine) axial coordination (*18*−*22* and see Table 1). However, the last of these three combinations gives rise to Gaussian, not asymmetric, band shapes (*18*, *22*, *32*) and is

Table 1: EPR and NIR MCD Properties of Low-Spin His/Met-Liganded Low-Spin Ferric Hemes

hemoprotein	EPR *g*-values[a]	wavelength (λ) and intensity ($\Delta\epsilon$) of NIR-CT MCD band[b] λ_{NIR-CT}/nm	$\Delta\epsilon$/M^{-1} cm^{-1}	ref
Ps. stutzeri cyt cd_1, heme *c*	2.97, 2.24, ~1.4	1775 (1775)	160 (0.8)	*23*
E. coli cyt b_{562}	3.03, 2.18, ~1.4	1860	175	*24*
horse heart cyt *c*	3.07, 2.23, 1.26	1750 (1725)	285 (0.8)	*25*
Ps. aeruginosa cyt c_{551}	3.20, 2.05, −	1800	330	*26*
E. coli cyt *bd*, heme b_{558}	3.32, −, −	1820	200	*27*
N. europeae cyt c_{552}	3.34, −, −	1800	340	*28*
SoxAX, heme-3	3.50, −, −	1900 (1800)	240 (0.84)	this work
cellobiose oxidase	~3.50, −, −	(1870)		*29*
Ps. stutzeri NOR, heme *c*	3.54, −, −	(1840)	(0.76)	*30*
Az. vinelandii cyt c_4	3.64, −, −	1900	~290	*31*
	3.22, −, −[c]			

[a] A dash indicates undetermined g_x or g_y values. [b] Values refer to data recorded at 4.2 K using 5 T magnetic field except where parentheses denote room-temperature measurements for which $\Delta\epsilon$ is expressed in units of M^{-1} cm^{-1} T^{-1}. [c] Cytochrome c_4 contains two types of histidine/methionine-liganded hemes with these g_z-values. Average MCD intensity is shown.

Table 2: EPR *g*-Values of Low-Spin Ferric Hemes with Thiolate as an Axial Ligand

heme species	g_z	g_y	g_x	axial ligands	ref
SoxA LS_{1a}	2.58	2.30	1.87	Cys^-/His	this work
SoxA LS_{1b}	2.52	2.23	1.84	Cys^-/His	this work
SoxA LS_2	2.42	2.26	1.91	?[a]	this work
cyt $P450_{cam}$ WT	2.45	2.26	1.91	Cys^-/H_2O	*37*
cyt P450 BM-3 WT	2.42	2.26	1.92	Cys^-/H_2O	*38*
nNOS WT	2.43	2.28	1.89	Cys^-/H_2O	*39*
human eNOS WT	2.45	2.30	1.87	Cys^-/H_2O	*40*
	2.42	2.30	1.90	Cys^-/H_2O	*41*
cyt $P450_{cam}$ + O-donor ligands	2.43−2.48	2.25−2.27	1.91−1.93	Cys^-/(O)	*37*
cyt $P450_{cam}$ + imidazole	2.56	2.27	1.87	Cys^-/Im	*37*
cyt P450 BM-3 + imidazole	2.61	2.25	1.83	Cys^-/Im	*38*
cyt P450 + imidazole derivatives	2.47−2.62	2.25−2.28	1.85−1.89	Cys^-/Im	*37*, *42*
chloroperoxidase + imidazole	2.53	2.28	1.85	Cys^-/Im	*43*
eNOS + imidazole, major at pH 8	2.70	2.30	1.75	Cys^-/Im	*40*
eNOS + imidazole, major at pH 6	2.57	2.30	1.83	Cys^-/Im	*40*
eNOS, major at pH 8	2.66	2.28	1.81	Cys^-/Im	*40*
+4-methylimidazole, major at pH 6	2.57	2.28	1.83	Cys^-/Im	*40*
eNOS + 1-(4-hydroxyphenyl)imidazole	2.57	2.30	1.84	Cys^-/Im	*41*
eNOS + 1-(3-aminopropyl)imidazole	2.61	2.29	1.80	Cys^-/Im	*41*
	2.54	2.29	1.80		*41*
CooA + Im	2.52	2.27	1.85	Cys^-/Im	*44*
myoglobin + HS^-	2.56	2.24	1.84	His/RS^-	*45*
	2.58	2.25	1.83	His/RS^-	*46*
cyt *c* M80C	2.56	2.27	1.85	Cys^-/His	*45*
chloroperoxidase + pyridine	2.58	2.29	1.84	Cys^-/(N)	*43*
human eNOS + pyridine	2.50	2.30	1.85	Cys^-/(N)	*40*
cyt $P450_{cam}$ + 2-phenylimidazole	2.41/2.45	2.25/2.27	1.91/1.92	Cys^-/PhIm	*37*
cyt $P450_{cam}$ + benzylimidazole	2.44	2.28	1.93	Cys^-/BenzIm	*37*
cyt $P450_{cam}$ + indole	2.41	2.26	1.93	Cys^-/Trp	*37*
human eNOS + lysine	2.58	2.28	1.82	Cys^-/(N)	*40*
cyt $P450_{cam}$ + 1-octylamine	2.49	2.26	1.89	Cys^-/amine	*42*
cyt $P450_{cam}$ + metyrapone	2.47	2.27	1.92	Cys^-/amine	*47*
CooA WT (major)	2.46	2.26	1.91	Cys^-/Pro(N)	*48*
CooA WT (minor)	2.58	2.26	1.85	Cys^-/Pro(N)	*44*, *48*

[a] Modified ligand set as described in text.

unlikely to be the ligand set of this particular low-spin species (hereafter LS_3). The intensity at 260−380 mT comprises two overlapping rhombic (or Type II) spectra with g_z-values of 2.42 (LS_2) and ~2.55 (LS_1). The latter shows structure indicative of a minor heterogeneity. Small differences in the power dependence of the signals (not shown) and variations in their relative intensities between different SoxAX preparations allow an assignment of the *g*-values to two spectra: LS_1 (g = ~2.55, 2.30, ~1.87) and LS_2 (g = 2.42, 2.25, 1.92). The g_z-value in a rhombic spectrum is always significantly lower than that of Large g_{max} cases, but in practice there are ligand-dependent limits to how low this value falls. For all known combinations of His, Lys, and Met ligands, the lowest g_z-value observed is 2.86 for bis-methionine (*33* and references cited therein). The g_z-values observed here for LS_1 and LS_2 are lower still, and there are few precedents for this. Alkaline globins have g_z = 2.57−2.51 (*34*, *35*), close to that of LS_1. However, g_y for these His/HO^--liganded hemes is 2.16−2.19, lower than the 2.30 observed here. Furthermore, these alkaline globins are always in thermal equilibrium

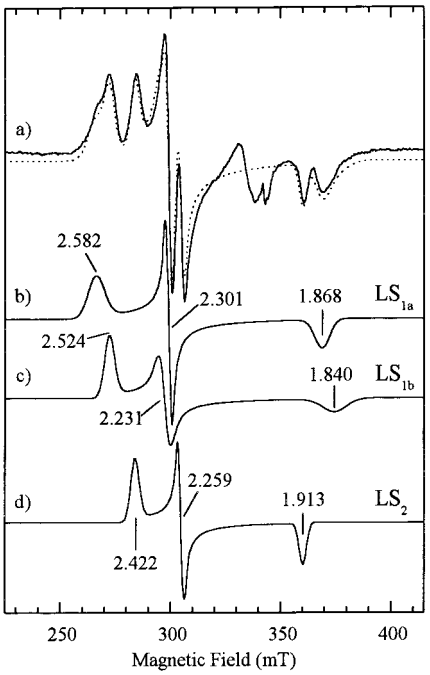

FIGURE 3: (a) X-band EPR spectrum in the low-spin ferric heme region of the as-prepared oxidized form of *R. sulfidophilum* SoxAX (—) and the simulated spectrum (•••) offset slightly for clarity. (b), (c), and (d) are the individual simulated spectra contributing to the simulation in (a).

between the high- and low-spin states (*36*), but the SoxAX electronic absorption and MCD spectra presented later show no characteristic high-spin transitions at any temperature. Extremely good matches for all three *g*-values of LS_1 and LS_2 are found only in the EPR of hemes for which one axial ligand is cysteinate, the properties of which dominate the spectrum. This EPR therefore provides compelling evidence that LS_1 and LS_2 have a cysteinate or similar thiolate axial ligand. It provides less information concerning the ligands trans to thiolate. Similar *g*-values to those of LS_1 have been reported for hemes with nitrogenous ligands distal to cysteinate (Table 2). These include the imidazole derivatives of P450, NOS and CPO, thiolate-bound globins, and the Met80Cys axial ligand variant of cytochrome *c*. However, nitrogenous ligands other than histidine are not completely ruled out. P450, ligated by several different amine derivatives, gives *lower* g_z-values (2.47−2.49), but lysine-liganded eNOS and metyrapone-bound cytochrome $P450_{NOR}$ have $g_z = 2.56-2.58$. One of the two EPR forms of oxidized CooA also has $g_z = 2.58$, and in this protein, the nitrogenous ligand trans to cysteinate was identified, somewhat unexpectedly, as the terminal proline residue (*44*, *49*−*51*). Thus, the EPR *g*-values indicate that LS_1 has a nitrogenous ligand distal to thiolate but do not identify this ligand. The LS_2 *g*-values are more ambiguous. They are typical of native P450 and NOS (Cys^-/water) and of adducts in which water is displaced by oxygen-donor ligands (Table 2). However, the *g*-values of the majority EPR species in oxidized CooA (Cys^-/Pro) are also very similar as are those of P450 when ligated by imidazole modified with various electron-withdrawing substituents (*37*).

Quantitation and Simulation of the EPR Signals of Oxidized SoxAX. The SoxAX low-spin heme EPR signals were quantitated using standard integration methods (*13*, *14*), showing that the 260−380 mT spectral envelope of LS_1 and

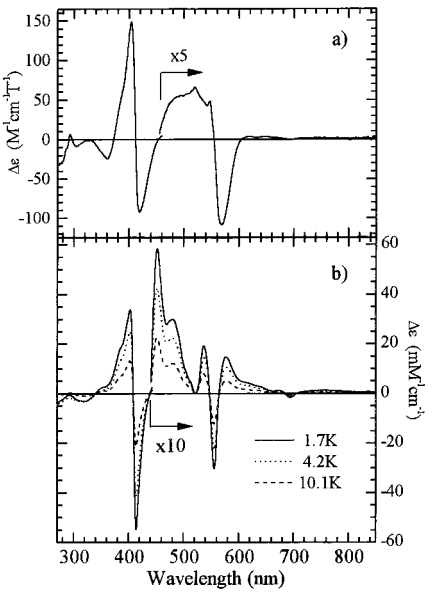

FIGURE 4: UV−visible MCD spectra of as-prepared oxidized *R. sulfidophilum* SoxAX. Buffers were as described under Materials and Methods. (a) Room-temperature MCD spectrum recorded using a magnetic field of 6 T. Sample concentrations used were 18 and 147 μM. (b) Low-temperature MCD spectra recorded using a magnetic field of 5 T and temperatures as shown. Sample concentrations used were 8 and 56 μM.

LS_2 accounts for ~2/3 of the total heme content and the $g = 3.50$ for the remaining heme. However, the LS_1 and LS_2 spectra do not appear to be of equivalent intensity, and so the relative contributions were determined by simulation using the method of Oganesyan (*52*) (Figure 3a). The minor heterogeneity of LS_1, evidenced by the structure on g_z, was accommodated by simulating three separate rhombic spectra, shown individually in Figure 3b−d, using an $LS_{1a}/LS_{1b}/LS_2$ ratio of 85/68/47 (expressed as percentages totalling 200). The total LS_1/LS_2 ratio for four samples of SoxAX varied between 154/46 and 105/95, but, significantly, it never fell below 100/100, suggesting that one heme (arbitrarily heme-1) remains in the LS_1 form whereas heme-2 can occur as an LS_1 or an LS_2 form. Note that this variation in the level of total LS_1 is not due simply to variations in the level of one of its components. This would require that either LS_{1a} or LS_{1b} remains at a level equivalent to one heme in all samples while the magnitude of the other varies inversely with that of LS_2. This is not observed. Rather, each of the hemes contributing to LS_1 has a split g_z feature. A similar small pH-dependent splitting of g_z has been observed for imidazole derivatives of NOS (*41*). The site of protonation was not identified. The pH dependence of SoxAX spectra is currently being investigated but is complicated by further changes in the EPR and MCD which occur following prolonged handling of the enzyme. These changes produce additional new spectroscopic features which are not observed in fresh samples and will not be discussed further here.

UV−Visible Region MCD of Oxidized SoxAX. In the RT UV−visible MCD spectrum of oxidized SoxAX (Figure 4a), the intense bands at 300−600 nm are characteristic of low-spin ferric heme. With combinations of His, Met, and Lys axial ligands, peak-to-trough Soret intensities are usually ~150 M^{-1} cm^{-1} T^{-1} (*50*). Heme-3 is in this category and will make the largest contribution to this band. Soret intensity for thiolate-liganded hemes is significantly weaker, typically

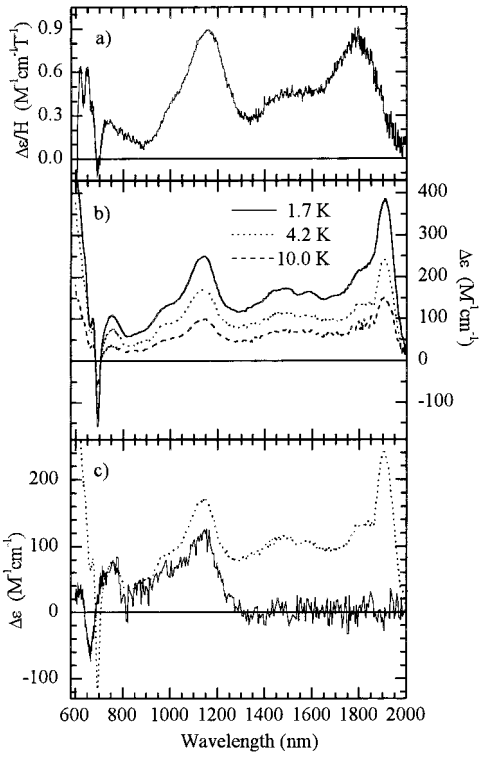

FIGURE 5: NIR MCD spectra of *R. sulfidophilum* SoxAX. Buffers were as described under Materials and Methods. (a) Room-temperature MCD spectrum of as-prepared oxidized form recorded using a magnetic field of 6 T and a sample concentration of 147 μM. (b) Low-temperature MCD spectra of as-prepared oxidized form recorded using a magnetic field of 5 T and temperatures as shown. Sample concentration was 56 μM. (c) MCD spectrum at 4.2 K (—) of dithionite-treated form recorded using a magnetic field of 5 T. Sample concentration was 55 μM. Also shown for comparison is a replot of the 4.2 K spectrum from (b) (···).

50−90 M^{-1} cm^{-1} T^{-1} (*37, 41, 53−58*). Thiolate coordination therefore explains a Soret intensity which, at 240 M^{-1} cm^{-1} T^{-1}, is relatively low for three low-spin hemes. The visible region (450−600 nm) is consistent with this; MCD α-bands are also weaker for thiolate coordination (*59*). The 300−600 nm region of the low-temperature MCD (Figure 4b) supports the above conclusions and furthermore shows no evidence for temperature-dependent spin or oxidation state changes. The few low-temperature MCD spectra reported for thiolate-bound hemes have Soret intensities, at 4.2 K, of 7−16 mM^{-1} cm^{-1} (*38, 44*), also much reduced compared to the 25−35 mM^{-1} cm^{-1} of other ligand sets. The SoxAX intensity is therefore again comparatively low due to thiolate ligation. Weak MCD intensity between 620 and 850 nm is expanded as part of Figure 5 and will be discussed below.

NIR MCD spectra of oxidized SoxAX are shown in Figure 5a,b. The well-resolved MCD bands at 600−800 nm correspond to weak shoulders in the absorption spectrum. No significant bands characteristic of high-spin ferric heme are observed. The minor trough at ∼631 nm at RT, if due to high-spin His/water coordination, would represent no more than ∼3% of one heme. The analogous transition for high-spin P450 and NOS, which occurs at ∼655 nm (see ref *41*), is not apparent here. These wavelengths are dominated by a sharp derivative feature centered at 685 nm with a trough at 695 nm. This is characteristic of His/Met coordination (*31, 60−62*).

At 800−2000 nm, these spectra contain positive features with intensities found only for the CT transition of low-spin ferric heme. The exact energy of this transition is diagnostic of the heme axial ligation (*44, 45*). Two such bands are immediately obvious in the MCD of SoxAX, at 1150 and 1900 nm (4.2 K), but there is also significant additional intensity in the region 1300−1700 nm. The 1900 nm band is unambiguously diagnostic of His/Met coordination and is of intensity consistent with one heme (see Table 1). The species responsible for the $g = 3.50$ EPR signal must give rise to a NIR-CT band, and this EPR feature is the only one which could arise from His/Met coordination. Therefore, the 685 and 1900 nm MCD bands are both due to heme-3. The prominent band at 1150 nm is thus the NIR-CT transition of one or more of the thiolate-bound hemes detected in the EPR. For imidazole-P450 and native CooA, both of which have a nitrogenous ligand distal to cysteinate, the CT transition is at 1180 nm (*38*) and 1120 nm (*44*), respectively. There is no peak in the SoxAX spectrum at the wavelength observed for native P450 (Cys^-/H_2O), 1080 nm (*38*). The 1150 nm band is therefore assigned to hemes with thiolate/nitrogen ligation and must account for at least the LS_1 species. NIR-CT MCD intensity is governed primarily by the relative energies of the ferric d-orbitals as is the form of the EPR spectrum (*63*). LS_1 *g*-values are similar to those of imidazole-P450, which has an NIR-CT MCD peak intensity of $\Delta\epsilon = 120$ M^{-1} cm^{-1} at 4.2 K (*38*). Thus, the 1150 nm band (170 M^{-1} cm^{-1}) must arise from more than one heme. Using the value of 120 M^{-1} cm^{-1} yields an estimate ∼1.42 hemes, in reasonable agreement with the figure of 1.53 for LS_1 derived from the EPR. Thus, LS_2, for which the second ligand is not identified, does not appear to contribute to the 1150 nm band. The only unassigned intensity remaining is at 1300−1700 nm, and this must be the CT intensity from LS_2. NIR-CT bands at these wavelengths have been observed for hemes with His/His (*45, 50, 64*) or His/Lys ligands (*22, 25, 65*). However, these combinations are already ruled out by the EPR. The $g_z = 3.50$ peak is the only EPR feature which could in principle arise from these ligand sets, but this has to be assigned to heme-3, shown unambiguously by MCD to have His/Met ligands. Furthermore, one of the LS_2 ligands must be a thiolate. Therefore, there is no known precedent for this combination of spectroscopic properties, and the LS_2 ligands cannot be unambiguously identified.

Dithionite-Reduced SoxAX. The sharp α-band at 551 nm in the absorption spectrum of dithionite-reduced SoxAX (Figure 1, dashed trace) would in principle be sufficient to account for three low-spin ferrous hemes (*66, 67*). However, the 4.2 K MCD of this sample (Figure 6) shows a characteristic sharp low-spin ferrous derivative shaped α-band at 548 nm but a low-spin ferric Soret band at 350−450 nm, indicating that reduction is incomplete. The sample was reclaimed from the MCD cryostat for EPR spectroscopy (Figure 2b) which showed that the only ferric species remaining is that with $g_z \sim 2.55$. The ferric Soret intensity is therefore due to unreduced LS_1 (the small sample volume makes EPR integration unreliable, and the MCD intensities are a better indication of the level of unreduced heme). Absence of the $g = 3.50$ EPR signal shows that heme-3 is fully reduced. The MCD α-band at 548 nm is almost identical to that of reduced cytochrome *c* (547 nm) (*59, 67*) as would be anticipated for heme-3 if it retains His/Met

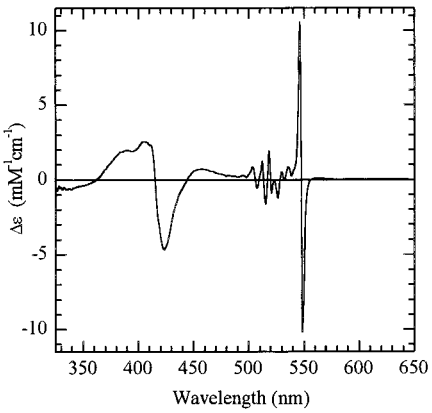

FIGURE 6: UV−visible MCD spectrum of the as-prepared dithionite-treated form of *R. sulfidophilum* SoxAX recorded at 4.2 K using a magnetic field of 5 T. Buffers were as described under Materials and Methods. Sample concentrations were 8 and 55 μM.

ligation upon reduction. But the band intensity is approximately twice that expected for one heme, and the feature shows no splitting. This implies that the second of the two reduced hemes now has similar coordination to that of heme-3, although hemes-1 and -2 had a thiolate ligand in the ferric state. The MCD α-band of ferrous CooA is at 555 nm, close to that of cytochrome b_5 (His/His, 557 nm) (*54*), but shifted from the region typical of thiolate ligation (562−567 nm) (*54*, *67*, *68*). This was taken to indicate reductive displacement of the cysteinate by a nitrogenous ligand (*44*). Since the effect on the spectrum of the thiolate ligand is unlike that of methionine, a similar phenomenon is suggested here for SoxAX. There are several possible interpretations: thiolate has been replaced by methionine; thiolate has been replaced by a residue to give a combination not previously characterized by MCD; or thiolate is protonated but retained as a thiol ligand in the reduced state [thiol is comparable in its effect on the spectrum to methionine or other thioethers (*67*, *68*)]. In the NIR MCD (Figure 5c, solid trace), the 695 and 1900 nm His/Met bands are absent, consistent with reduction of heme-3. The intensity at 1300−1700 nm has completely disappeared whereas the Cys^-/N 1150 nm band is diminished to ∼120 M^{-1} cm^{-1}, approximately that expected for one heme.

CONCLUSIONS

The three *c*-type hemes of oxidized SoxAX are low spin. Heme-3 is responsible for a Large g_{max} EPR signal and has His/Met ligands. We infer that heme-3 is bound to SoxX and axially ligated by Met92 (*R. sulfidophilum* numbering), the only invariant methionine residue (*6*), and by His46 of the single heme attachment motif in this subunit. Heme-1 and heme-2 are associated with SoxA, and each has a thiolate ligand in the oxidized state. Both can occur in a form giving rise to an LS_1 EPR spectrum and an MCD band near 1150 nm, the spectroscopic properties of heme with a nitrogenous ligand distal to cysteinate. It can be assumed that the nitrogen ligand is the histidine of the two SoxA heme attachment motifs (His80 and His181) and then that the cysteinate ligands are the conserved residues Cys114 and Cys222 (*6*). A preparation-dependent fraction of heme-2 is found in a modified form which gives rise to the LS_2 EPR spectrum. When SoxAX is treated with the reductant dithionite, the His/Met-ligated heme-3 is reduced to the low-spin ferrous state with retention of ligands. The Cys^-/His heme-1 remains oxidized. Heme-2, which displays variable LS_1/LS_2 heterogeneity in oxidized protein, is reduced to the low-spin ferrous state. However, the UV−visible MCD is not consistent with the presence of a cysteinate ligand to reduced heme-2. Instead, thiolate has been either protonated and retained as a thiol ligand or replaced by an alternative coordinating group. The spectrum rules out histidine and lysine as the replacement, and the sequence makes methionine unlikely as SoxA does not contain a conserved methionine residue (*6*).

The nature of the ligand in the LS_2 heme species is not determined by these studies. The *g*-values are ambiguous, but the red-shift of the NIR MCD CT band relative to that of Cys^-/His at 1150 nm points to an axial ligand pair with a lower crystal-field strength. It is unlikely that the His ligand of the heme binding motif of LS_2 has been chemically modified or replaced. However, if the unknown LS_2 thiolate ligand is more electron-withdrawing than unmodified Cys^-, then this could account for the NIR MCD since the NIR-CT band energy reflects the separation between the porphyrin HOMOS and the ferric d-orbital manifold and is determined primarily by ligand basicity. We therefore propose that LS_2 is coordinated by His and a thiolate species that is derived either from chemical modification of the cysteinate or from its substitution with an exogenous thiolate ligand. Exogenous sulfide or alkanethiolate is ruled out because this would give NIR-CT bands at 1000−1200 nm (*45*). Cysteine residues oxidized to the level of sulfenate ($R-S-O^-$) or sulfinate ($R-SOO^-$) are known to occur in proteins, and both are metal ion ligands in non-heme iron and cobalt-containing nitrile hydratases (*69*). However, this degree of modification at the sulfur atom makes it unlikely that coordination of these species to heme iron would result in the EPR spectra typical of thiolate ligation. The spectroscopic properties of LS_2 could be accounted for by conjugation of the cysteine sulfur atom to one or more further sulfur atoms. Examples would be thiosulfate ($^-S-SO_3^-$), polysulfides ($^-S-(S)_n-S^-$), or cysteine-based S^0 conjugates such as cysteine sulfane (Cys-S−S^-). For these ligands, partial delocalization of the ligand charge over additional sulfur would constitute the electron-withdrawing effect responsible for the long-wavelength of the MCD NIR-CT band of LS_2. The apparent mass of SoxA, from electrospray mass spectrometry, was 35 ± 4 Da greater than that expected from the gene sequence plus the mass of two hemes (*6*). This addition could represent the additional sulfur atom of cysteine sulfane. The iron−sulfur cluster of *D. vulgaris* prismane protein (*70*) provides a precedent for cysteine sulfane as an iron ligand in biology. We note, however, that long-chain polysulfides can be cleaved under relatively mild conditions to leave cysteine sulfane (*71*), and it cannot be ruled out that this such a modification is occurring during mass spectrometry of SoxAX.

Basic EPR spectra have previously been reported for one other member of the SoxAX family, the cytochrome $c_{552.5}$ of *Paracoccus versutus* (*7*). These show four different low-spin ferric heme signatures which, on the basis of nearly identical *g*-values, correlate directly with the hemes described in this work. Although not discussed in ref *11*, the relative levels of the hemes with $g_z \sim 2.55$ and $g_z \sim 2.43$ are significantly different in two spectra of what is apparently the same form of oxidized cytochrome $c_{552.5}$ recorded under

identical conditions. Crucially, the two forms appear to be present at comparable levels in one spectrum whereas in a second the $g_z \sim 2.43$ form is much reduced relative to the $g_z \sim 2.55$.

Most thiolate-liganded hemoproteins are P450s or related enzymes, such as NOS and CPO, and have Cys^-/H_2O-bound ferric *b*-type heme at the active site. CooA and human cystathionine β-synthase also contain Cys^--liganded *b*-type heme, but both have been shown to have a nitrogenous second ligand, a terminal proline residue in the case of CooA. Cystathionine β-synthase was suggested to be the first example of Cys^-/His ligation (*72*). The rat protein H450, recognized for some years to contain thiolate-liganded heme, is now known to be equivalent to cystathionine β-synthase (*56*, *73*). Thus SoxAX is the first protein shown to contain *c*-type heme with a cysteinate ligand and is one of only two known examples of naturally occurring Cys^-/His coordination. In addition, SoxAX contains a heme with a novel modified thiolate ligand. The unusual coordination of the two SoxA hemes is likely to be of functional importance and reinforces the idea that SoxAX has an enzymatic rather than solely electron-transfer function.

ACKNOWLEDGMENT

We thank J. Mayne, J. Thornton, and D. Clarke for assistance in cell culture and protein purification; Dr. Vasily Oganesyan for the EPR simulations; and Dr. Andrew Hemmings and Prof. Andrew Thomson for helpful discussions and critical reading of the manuscript.

REFERENCES

1. Brune, D. C. (1995) in *Anoxygenic Photosynthetic Bacteria* (Blankenship, R. E., Madigan, M. T., and Bauer, C. E., Eds.) pp 847−870, Kluwer Academic Publishers, Dordrecht, The Netherlands.
2. Friedrich, C. G., Quentmeier, A., Bardischewsky, F., Rother, D., Kraft, R., Kostka, S., and Prinz, H. (2000) *J. Bacteriol. 182*, 4677−4687.
3. Petri, R., Podgorsek, L., and Imhoff, J. F. (2001) *FEMS Microbiol. Lett. 197*, 171−178.
4. Klarsov, K., Verté, F., Van Driessche, G., Meyer, T. E., Cusanovich, M. A., and Van Beeumen, J. (1998) *Biochemistry 37*, 10555−10562.
5. Mukhopadhyaya, P. N., Deb, C., Lahiri, C., and Roy, P. (2000) *J. Bacteriol. 182*, 4278−4287.
6. Appia-Ayme, C., Little, P. J., Matsumoto, Y., Leech, A. P., and Berks, B. C. (2001) *J. Bacteriol*. (in press).
7. Kelly, D. P., Shergill, J. K., Wei-Ping, L., and Wood, A. P. (1997) *Antonie van Leeuwenhoek 71*, 95−107.
8. Wodara, C., Kostka, S., Egert, M., Kelly, D. P., and Friedrich, C. G. (1994) *J. Bacteriol. 176*, 6188−6191
9. Kusai, K., and Yamanaka, T. (1973) *Biochim. Biophys. Acta 325*, 304−314
10. Lu, W.-P., and Kelly, D. P. (1984) *Biochim. Biophys. Acta 765*, 106−117.
11. Thomson, A. J., Cheesman, M. R., and George, S. J. (1993) *Methods Enzymol. 226*, 199−232
12. Berry, E. A., and Trumpower, B. L. (1987) *Anal. Biochem. 161*, 1−15.
13. Aasa, R., and Vängård, T. (1975) *J. Magn. Reson. 19*, 308−315.
14. De Vries, S., and Albracht, S. P. J. (1979) *Biochim. Biophys. Acta 546*, 334−340.
15. Oganesyan, V. S., Butler, C. S., Watmough, N. J., Greenwood, C., Thomson, A. J., and Cheesman, M. R. (1998) *J. Am. Chem. Soc. 120*, 4232−4233.
16. Walker, F. A. (1999) *Coord. Chem. Rev. 186*, 471−534.
17. Walker, F. A., Huynh, B. H., Scheidt, W. R., and Osvath, S. R. (1986) *J. Am. Chem. Soc. 108*, 5288−5297.
18. Siedow, J. N., Vickery, L. E., and Palmer, G. (1980) *Arch. Biochem. Biophys. 203*, 101−107.
19. Hederstedt, L., and Andersson, K. K. (1986) *J. Bacteriol. 167*, 735−739.
20. Fridén, H., Cheesman, M. R., Hederstedt, L., Andersson, K. K., and Thomson, A. J. (1990) *Biochim. Biophys. Acta 1041*, 207−215.
21. Berry, M. J., George, S. J., Thomson, A. J., Santos, H., and Turner, D. L. (1990) *Biochem. J. 270*, 413−417.
22. Rigby, S. E. J., Moore, G. R., Gray, J. C., Gadsby, P. M. A., George, S. J., and Thomson, A. J. (1988) *Biochem. J. 256*, 571−577.
23. Cheesman, M. R., Ferguson, S. J., Moir, J. W. B., Richardson, D. J., Zumft, W. G., and Thomson, A. J. (1997) *Biochemistry 36*, 16267−16276.
24. Moore, G. R., Williams, R. J. P., Peterson, J., Thomson, A. J., and Matthews, F. S. (1985) *Biochim. Biophys. Acta 829*, 83−96.
25. Gadsby, P. M. A., Peterson, J., Foote, N., Greenwood, C., and Thomson, A. J. (1987) *Biochem. J. 246*, 43−54.
26. Foote, N., Peterson, J., Gadsby, P. M. A., Greenwood, C., and Thomson, A. J. (1984) *Biochem. J. 223*, 369−378.
27. Spinner, F., Cheesman, M. R., Thomson, A. J., Kaysser, T., Gennis, R. B., Peng, Q., and Peterson, J. (1995) *Biochem. J. 308*, 641−644.
28. Arciero, D. M., Peng, Q., Peterson, J., and Hooper, A. B. (1994) *FEBS Lett. 342*, 217−220.
29. Cox, M. C., Rogers, M. S., Cheesman, M., Jones, G. D., Thomson, A. J., Wilson, M. T., and Moore, G. R. (1992) *FEBS Lett. 307*, 233−236.
30. Cheesman, M. R., Zumft, W. G., and Thomson, A. J. (1998) *Biochemistry 37*, 3994−4000.
31. Gadsby, P. M. A., Hartshorn, R. T., Moura, J. J. G., Sinclair-Day, J. D., Sykes, A. G., and Thomson, A. J. (1989) *Biochim. Biophys. Acta 994*, 37−46.
32. Gadsby, P. M. A., and Thomson, A. J. (1986) *FEBS Lett. 197*, 253−257.
33. Cheesman, M. R., Kadir, F. H. A., Al-Basseet, J., Al-Massad, F., Farrar, J., Greenwood, C., Thomson, A. J., and Moore, G. R. (1992) *Biochem. J. 286*, 361−367.
34. Gurd, F. R. N., Falk, K., Malmström, B. O., and Vänngård, T. (1967) *J. Biol. Chem. 242*, 5724−5730.
35. Maskall, C. S., Gibson, J. F., and Dart, P. J. (1977) *Biochem. J. 167*, 435−445.
36. George, P., Beetlestone, J., and Griffith, J. S. (1964) *Rev. Mod. Phys. 36*, 441−463.
37. Dawson, J. H., Andersson, L. A., and Sono, M. (1982) *J. Biol. Chem. 257*, 3606−3617.
38. McKnight, J., Cheesman, M. R., Thomson, A. J., Miles, J. S., and Munro, A. W. (1993) *Eur. J. Biochem. 213*, 683−687.
39. Salerno, J. C., Frey, C., McMillan, K., Williams, R. F., Masters, B. S. S., and Griffith, O. W. (1995) *J. Biol. Chem. 270*, 27423−27428.
40. Tsai, A.-L., Berka, V., Chen, P.-F., and Palmer, G. (1996) *J. Biol. Chem. 271*, 32563−32571.
41. Berka, V., Palmer, G., Chen, P.-F., and Tsai, A. L. (1998) *Biochemistry 37*, 6136−6144.
42. Ruf, H. H., Wende, P., and Ullrich, V. (1979) *J. Inorg. Biochem. 11*, 189−204.
43. Sono, M., Hager, L. P., and Dawson, J. H. (1991) *Biochim. Biophys. Acta 1078*, 351−359.
44. Dhawan, I. K., Shelver, D., Thorsteinsson, D., Roberts, G. P., and Johnson, M. K. (1999) *Biochemistry 38*, 12805−12813.
45. Gadsby, P. M. A., and Thomson, A. J. (1990) *J. Am. Chem. Soc. 112*, 5003−5011.
46. Berzofsky, J. A., Peisach, J., and Blumberg, W. E. (1971) *J. Biol. Chem. 246*, 3367−3377.
47. Peterson, J. A., Ullrich, V., and Hildenbrandt, A. G. (1971) *Arch. Biochem. Biophys. 145*, 531−542.

48. Shelver, D., Thorsteinsson, M. V., Kerby, R. L., Chung, S.-Y., Roberts, G. P., Reynolds, M. F., Parks, R. B., and Burnstyn, J. N. (1999) *Biochemistry 38*, 2669−2678.
49. Lanzilotta, W. N., Schuller, D. J., Thorsteinsson, M. V., Kerby, R. L., Roberts, G. P., and Poulos, T. L. (2000) *Nat. Struct. Biol. 7*, 876−880.
50. Cheesman, M. R., Greenwood, C., and Thomson, A. J. (1991) *Adv. Inorg. Chem. 36*, 201−255.
51. Shelver, D., Kerby, R. L., He, Y., and Roberts, G. P. (1997) *Proc. Natl. Acad. Sci. U.S.A. 94*, 11216−11220.
52. Hunter, D. J. B., Oganesyan, V. S., Salerno, J. C., Butler, C. S., Ingledew, W. J., and Thomson, A. J. (2000) *Biophys. J. 78*, 439−450.
53. Shimizu, T., Nozawa, T., Hatano, M., Imai, Y., and Sato, R. (1975) *Biochemistry 14*, 4172−4178.
54. Vickery, L., Salmon, A., and Sauer, K. (1975) *Biochim. Biophys. Acta 386*, 87−98.
55. Dawson, J. H., Sono, M., and Hager, L. P. (1983) *Inorg. Chim. Acta 79*, 184−186.
56. Svastits, E. W., Alberta, J. A., Kim, I.-C., and Dawson, J. H. (1989) *Biochem. Biophys. Res. Commun. 165*, 1170−1176.
57. Sigman, J. A., Pond, A. E., Dawson, J. H., and Lu, Y. (1999) *Biochemistry 38*, 11122−11129.
58. Rux, J. J., and Dawson, J. H. (1991) *FEBS Lett. 290*, 49−51.
59. Vickery, L., Nozawa, T., and Sauer, K. (1976) *J. Am. Chem. Soc. 98*, 351−357.
60. Schejter, A., and George, P. (1964) *Biochemistry 3*, 1045−1049.
61. Moore, G. R., Williams, R. J. P., Peterson, J., Thomson, A. J., and Mathews, F. S. (1985) *Biochim. Biophys. Acta 829*, 83−96.
62. Arciero, D. M., Peng, Q., Peterson, J., and Hooper, A. B. (1994) *FEBS Lett. 342*, 217−220.
63. Thomson, A. J., and Gadsby, P. M. A. (1990) *J. Chem. Soc., Dalton Trans.*, 1921−1928.
64. Dawson, J. H., and Dooley, D. M. (1989) in *Physical Bioinorganic Chemistry Series, Iron Porphyrins Part II* (Lever, A. B. P., and Gray, H. B., Eds.) Chapters 1 and 2, VCH Publishers, Inc., New York.
65. Simpkin, D., Palmer, G., Devlin, F. J., McKenna, M. C., Jensen, G. M., and Stephens, P. J. (1989) *Biochemistry 28*, 8033−8039.
66. Moore, G. R., and Pettigrew, G. W. (1987) in *Cytochromes c: Biological Aspects*, Springer-Verlag, New York.
67. Dawson, J. H., Andersson, L. A., and Sono, M. (1983) *J. Biol. Chem. 258*, 13637−13645.
68. Sono, M., Andersson, L. A., and Dawson, J. H. (1982) *J. Biol. Chem. 257*, 8308−8320.
69. Claiborne, A., Yeh, J. I., Mallett, T. C., Luba, J., Crane, E. J., III, Charrier, V., and Parsonage, D. (1999) *Biochemistry 38*, 15407−15416.
70. Arendsen, A. F., Hadden, J., Card, G., McAlpine, A. S., Bailey, S., Zaitsev, V., Duke, E. H. M., Lindley, P. F., Kröckel, M., Trautwein, A. X., Feiters, M. C., Charnock, J. M., Garner, C. D., Marritt, S. J., Thomson, A. J., Kooter, I. M., Johnson, M. K., van den Berg, W. A. M., van Dongen, W. M. A. M., and Hagen, W. R. (1998) *J. Biol. Inorg. Chem. 3*, 81−95.
71. Klimmek, O., Stein, T., Pisa, R., Simon, J., and Kröger, A. (1999) *Eur. J. Biochem. 263*, 79−84.
72. Ojha, S., Hwang, J., Kabil, Ö., Penner-Hahn, J. E., and Banerjee, R. (2000) *Biochemistry 39*, 10542−10547.
73. Omura, T., Sadano, H., Hasegawa, T., Yoshida, Y., and Kominami, S. (1984) *J. Biochem. 96*, 1491−1500.

BI0100081